ECS Transactions, 75 (15) 575-583 (2016)
10.1149/07515.0575ecst ©The Electrochemical Society

Conductivity Maxima vs. Temperature: Grotthuss Conductivity in Aprotic Molten Salts

N. P. Aravindakshan, C. M. Kuntz, K. E. Gemmell, K. E. Johnson, and A. L. L. East

Department of Chemistry and Biochemistry, University of Regina, Regina, SK, S4S 0A2, Canada.

The phenomenon of electrical conductivity maxima of molten salts versus temperature during orthobaric (closed-vessel) conditions is further examined. First, we summarize results from density-functional-based molecular dynamics simulations of molten $SnCl_2$ and $HgBr_2$, which provided structural information but also succeeded in reproducing (i) previously published experimental conductivities to within an order of magnitude, and (ii) the conductivity maxima. The "hopping" mechanism we previously proposed is now termed a Grotthuss mechanism, which became quite clear in the simulations of the molecular liquid $HgBr_2$ which exhibited Grotthuss chains of bromide transfers. Second, we fit the experimental conductivities of 12 different molten salts with the equation $\sigma = e^{-aT}e^{b}e^{-c/T}$, which fits well in most cases, and mapped the density-dependent Arrhenius equation $\sigma(T,\rho) = A(\rho)e^{-Ea(\rho)/RT}$ onto it in a particular way, generating A and E_a curves for each molten salt for physical insight.

Introduction

In the 1960s, Yosim and Grantham studied the electrical conductivities of several "covalent" molten salts, such as CuCl, $BiCl_3$, $SnCl_2$, and $HgBr_2$, at elevated temperatures under orthobaric conditions (sealed under vacuum) (1-4). They found that there is a maximum in specific conductivity vs temperature for at least 11 of these. They attributed the conductivity decline at high temperatures to increased ion association (loss of ions), which they related to the falling density. Others, e.g. Janz (5) and Todheide (6) presented the hypothetical ion association as a shift in ion/molecule equilibria, e.g.

$$2BiCl_3 \rightleftharpoons BiCl_2^+ + BiCl_4^- \qquad [1]$$

as is done with partial ionizations in aqueous solution.

We first questioned the existence of such ion/molecule equilibria in 2012 when our simulations of molten $BiCl_3$ using density-functional-theory (DFT) forces showed no identifiable molecules, but a network liquid instead (7). We instead put forward a new theory to explain the conductivity maximum vs temperature (7, 8). The new theory attributed conductivity to atomic ions "hop[ping] from counterion to counterion," and used a density-dependent Arrhenius equation:

$$\sigma(T,\rho) = A(\rho)e^{-Ea(\rho)/RT} \quad [2]$$

to ascribe the maximum to the competing effects of rising hopping opportunities (rising frequency factor A with thermal expansion) and diminishing hopping probability per opportunity (due to rising activation energy E_a as the hopping distance increases with thermal expansion). An initial attempt to map this equation onto experimental data of several molten salts was made (8), using a crude first-principles equation for A(ρ) and deriving the resulting $E_a(\rho)$, but no functional form for $E_a(\rho)$ was provided, and it was not known if the results should be deemed realistic.

Here we provide a preliminary Communication of results from simulations of molten $SnCl_2$ and molten $HgBr_2$ at 6 different temperatures, with a full paper to be published elsewhere. These simulations were chosen to see if conductivity maxima could be reproduced for liquids other than $BiCl_3$, choosing a salt of similar conductivity ($SnCl_2$, σ_{max} = 2.81 Ω^{-1} cm^{-1}) and one of much lower conductivity ($HgBr_2$, σ_{max} = 4.06 x 10^{-4} Ω^{-1} cm^{-1}), and to see if the liquid structures in both cases still support the conjectured ideas of a rising A and rising E_a as the liquids thermally expand. We also add a new analysis of the known experimental orthobaric conductivities of a dozen molten halide salts.

Methodology

Ab initio molecular dynamics simulations (AIMD) were performed as before (7) using Vienna Ab-initio Simulation Package (VASP) software (9, 10), with its potpawGGA plane-wave basis sets (11, 12), standard precision (PREC = NORMAL), ENMAX = 400 eV, isotope-averaged masses, a Nosé thermostat for canonical-ensemble (NVT) conditions (13) with 40 fs thermal oscillations (SMASS = 0), and a Verlet velocity algorithm (14). For forces the PW91 level of density functional theory was used (15) with an added Grimme-style van-der-Waals (vdW) attractive potential (16).

The liquids were simulated at six different temperatures in cubic cells consisting of 120 atoms ($M_{40}X_{80}$), which are replicated using periodic boundary conditions. The cell sizes were chosen to fit orthobaric densities given by Janz (17). Over 70000 timesteps were performed at each temperature, using steps τ = 6 fs for $HgBr_2$ and 4 fs for $SnCl_2$. The simulation movies were viewed and analysed using VMD software (18).

Specific conductivities (σ) were calculated using the Einstein formula

$$\sigma^{Ein} = \frac{1}{VkT}\lim_{t\to\infty} ein_\sigma(t),\ ein_\sigma(t) = \frac{\langle|\vec{M}(t)-\vec{M}(t_0)|^2\rangle}{6t} \quad [3]$$

where $\vec{M}(t)$ is the total electric dipole of the simulation cell at time t, V is the volume of the cell, T is temperature in Kelvin, and ‹› denote averaging over all choices of t_0. Atom diffusion constants were also computed (and rise steadily with T); these are reported in the full paper. Further details, including the extrapolation techniques used to obtain the limit in Eq 3, will appear in the full paper.

Results and Discussion

Data from Simulations

Nature of molten $SnCl_2$. Molten $SnCl_2$ is a *network covalent liquid* as seen from the simulations. The chlorides are largely bridging, but show moments of single coordination, and small but frequent hops between metal cations. The Sn-Cl radial distribution (Figure 1) shows strong overlap of the singly-coordinate-Cl peak (2.6 Å) with the bridging-Cl peak (3.2 Å). The radial distribution also features a gradual shift of in the first peak towards lower bond length with rise in temperature. Thus this liquid is structurally similar to molten $BiCl_3$ (7). Integrating the g(r) functions out to 4.1 Å produces 6-coordinate Sn and 3-coordinate Cl in this network melt; integration out to only 2.8 A produces 2-coordinate Sn and 1-coordinate Cl. Much of this we knew from a single-temperature simulation of $SnCl_2$ we had already performed (8).

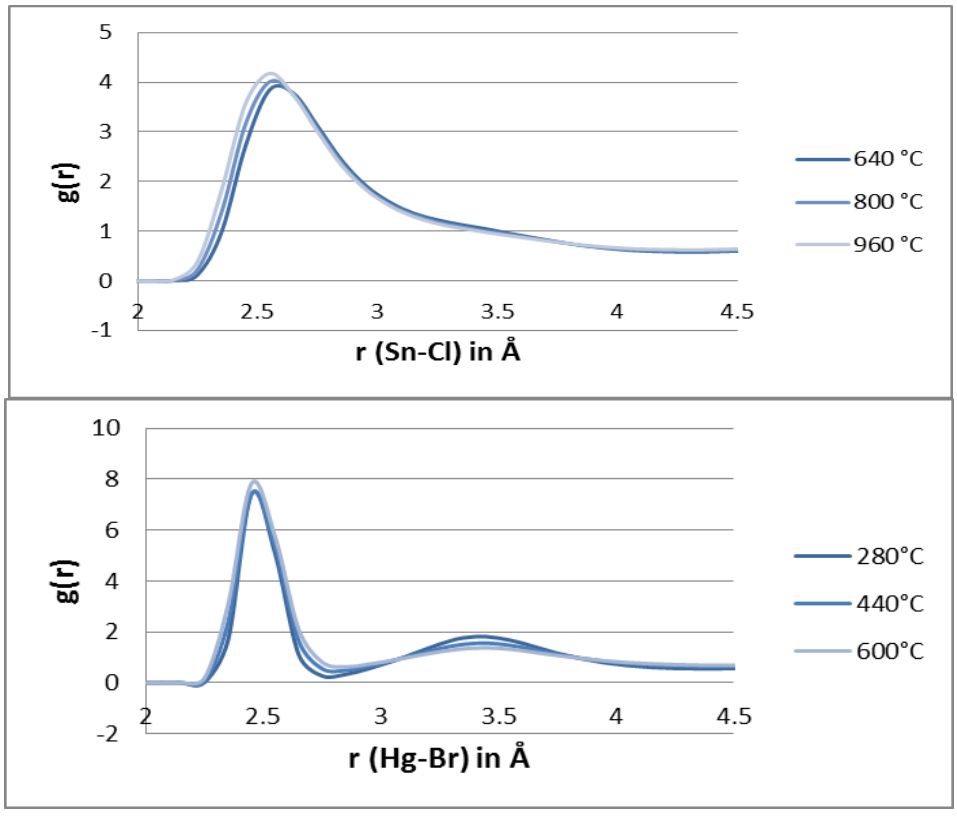

Figure 1. M-X radial distributions from simulations of molten $SnCl_2$ (top) and $HgBr_2$ (bottom).

Nature of molten $HgBr_2$. Molten $HgBr_2$ is a *molecular covalent liquid* consisting of linear triatomic molecules, as seen from the simulations. It undergoes frequent dimeric collisions (one every 5 ps), some of which result in metathesis-like concerted bromine exchanges. The Hg-Br radial distribution (Figure 1) shows a *distinct* peak for singly-coordinate Br (2.5 Å), with a second peak at 3.4 Å for an intermolecular Hg…Br distance. Unlike in $SnCl_2$ there is no drift of the peak position with temperature. An analysis of the molecular entities present in the simulations revealed (i) a variety of neutral and ionic species at small concentrations, including oligomers, but all of these having exceedingly short lifetimes (~40 fs for $HgBr^+$), (ii) a degree of ionisation (α) in the order of 10^{-2}, about 100 times larger than the poor estimate of Janz, 2 x 10^{-4} (19, 20), (iii) a degree of ionization that rises with T, violating the assumed rule of thumb of increased "ion association" past the conductivity maximum, and (iv) clear chains of *Grotthuss relays of bromide transfer* (Figure 2).

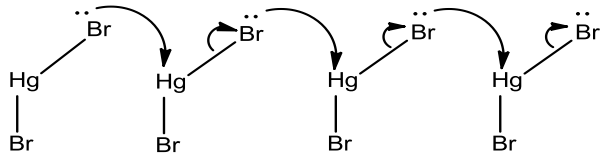

Figure 2. The Grotthuss relay observed in molten $HgBr_2$ simulations.

Specific Conductivities. Table I summarizes the conductivities for $SnCl_2$ and $HgBr_2$ calculated from the simulations. The specific conductivity maxima versus temperature are qualitatively reproduced for both liquids, and match the differing order of magnitudes for the two salts. A systematic error that decreases with increasing T may be present in the data of the low-conducting molecular liquid ($HgBr_2$). It is perhaps remarkable that the $HgBr_2$ simulations were able to reproduce the small conductivity values as well as they did. For both salts, the qualitative and semiquantitative reproduction of the conductivity maxima lends strong support to the realism of the simulations.

TABLE I. Specific conductivities from simulation (σ^{Ein}). Experimental values are from interpolation of data from Ref. 2.

$SnCl_2$			$HgBr_2$		
T (°C)	**σ^{Ein} (S cm^{-1})**	**σ^{expt} (S cm^{-1})**	**T (°C)**	**σ^{Ein} (S cm^{-1})**	**σ^{expt} (S cm^{-1})**
560	2.4	2.33	280	0.00173	0.00022
640	3.0	2.54	360	0.00208	0.00035
720	3.3	2.70	440	0.00184	0.00040
800	3.8	2.77	520	0.00111	0.00036
880	4.4	2.82	600	0.00055	0.00024
960	2.5	2.77	680	0.00004	0.00004

Fitting to Known Experimental Data

Inspection of the molecular movies suggested to us that the reasons for the conductivity falloff past the maximum are due to inhibited Grotthuss mobility, and might be due to a rising E_a in the case of $SnCl_2$ but a falling frequency factor A in the case of $HgBr_2$. That the mechanism has now been identified as a Grotthuss one has helped, but we have yet to find the best way of mapping Eq. 2 onto experimental data. (to determine $A(\rho)$ and $E_a(\rho)$ values). This time, instead of starting with an attempted first-principles equation for $E_a(\rho)$ (7) or for $A(\rho)$ (8), we began with the trial-and-error discovery that the 3-parameter

$$\sigma = e^{-aT} e^{b} e^{-c/T} \qquad [4]$$

function happens to fit the conductivity data for several molten salts exceptionally well (Figures 3 and 4). Only for the peculiar case of HgI_2 (conductivities always descending as T rises) does the function appear approximate. Practitioners may find this fitting function to be useful.

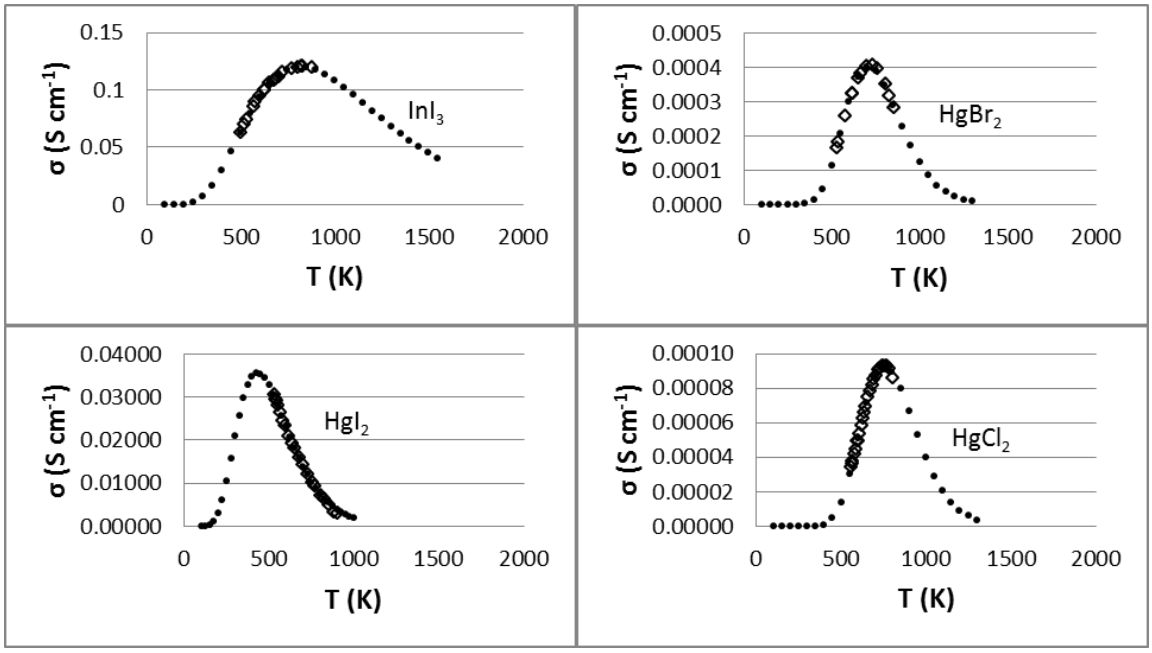

Figure 3. Fits (solid dots) of Eq. 4 to experimental data (open diamonds) for four salts which are likely *molecular* in nature. Expt. data from Ref. 2.

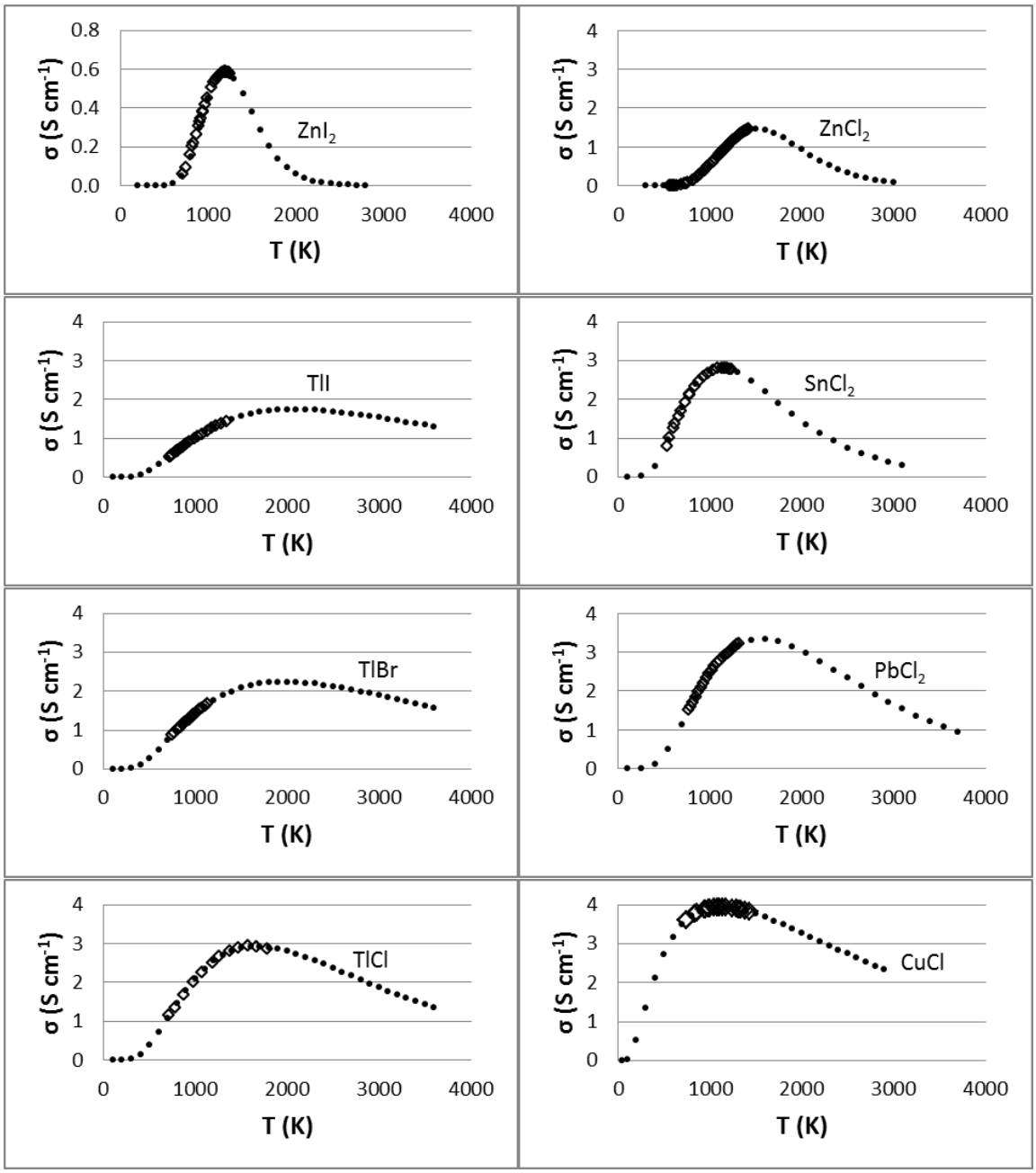

Figure 4. Fits (solid dots) of Eq. 4 to experimental data (open diamonds) for eight salts which are likely *network (bridging-halide)* in nature. Expt. data from Ref. 2, except Ref. 21 for $ZnCl_2$ and Ref. 22 for TlCl.

It is still not clear how to best map the Arrhenius equation (Eq. 2) onto the experimental data (represented almost exactly by Eq. 4). Equating the natural logs of both equations results in

$$-aT + b - cT^{-1} = \ln A - E_a R^{-1} T^{-1} \quad [5]$$

We present our best current idea. To accommodate a wide range of molten salts we chose to write

$$\ln A = d_0 + d_1 T \quad [6]$$

$$E_a = \varepsilon_0 + \varepsilon_1 T + \varepsilon_2 T^2 \quad [7]$$

with the understanding that the A and E_a are meant to be direct functions of *density*, and only *indirect* functions of temperature here (due to the thermal expansion: density falls reasonably linearly as temperature rises). Thus Eq. 5 becomes

$$\begin{aligned} -aT + b - cT^{-1} &= d_0 + d_1 T - \varepsilon_0 R^{-1} T^{-1} - \varepsilon_1 R^{-1} - \varepsilon_2 R^{-1} T \\ -aT + b - cT^{-1} &= (d_1 - \varepsilon_2 R^{-1}) T + (d_0 - \varepsilon_1 R^{-1}) - \varepsilon_0 R^{-1} T^{-1} \end{aligned} \quad [8]$$

and thus we need means of apportioning *a* amongst $\{d_1,\varepsilon_2\}$, and *b* amongst $\{d_0,\varepsilon_1\}$. The apportioning may depend on the melt: for molecular melts we expect A to be falling and E_a somewhat level, while for network melts we expect A to be level and E_a to be rising. Conductivity itself could be a rough metric of the molecularity of the melt (the mercuric halides certainly have low conductivity), and hence we made the choices

$$d_0 = (-0.9\sigma_{\max}^{1/3} + 1.5)b \quad [9a]$$

$$d_1 = (+2.8\sigma_{\max}^{1/3} - 1.3)a \quad [9b]$$

With these, the epsilons are obtained via Eq. 8:

$$\varepsilon_0 = cR \quad [9c]$$

$$\varepsilon_1 = (d_0 - b)R \quad [9d]$$

$$\varepsilon_2 = (d_1 + a)R \quad [9e]$$

The recipe is thus: one takes the experimental conductivities versus temperature for a melt, fits Eq 4 to obtain {a, b, c} as well as σ_{max}, and uses these in Eqs. 9a-e to obtain the coefficients needed for Eqs. 6 (for A) and 7 (for E_a).

The results of this recipe for the 12 melts in Figures 3 and 4 appear in Figure 5 and Table II. To our eye the results seem reasonable except for the zinc halides, whose A and E_a values seem too high for a network melt. We note that molten $ZnCl_2$ is particularly viscous (the viscosity of ZnI2 is unknown), but it is not apparent why this viscosity would lead to high activation energies for Grotthuss conductivity. We instead suspect that the zinc salts must need a different apportioning, which could lower both A and E_a.

In closing, although the choice of mapping of Eq. 2 onto Eq. 4 (particularly the choices of Eqs. 9a and 9b) were made according to our chemical intuition, the resulting A

and E_a functions are in agreement with the idea that the conductivity falloff (causing the maxima) are due to lowered mobility of ions, due to a falling collision frequency factor A for particularly molecular melts ($HgCl_2$ and $HgBr_2$) but a rising hopping barrier E_a for network halides.

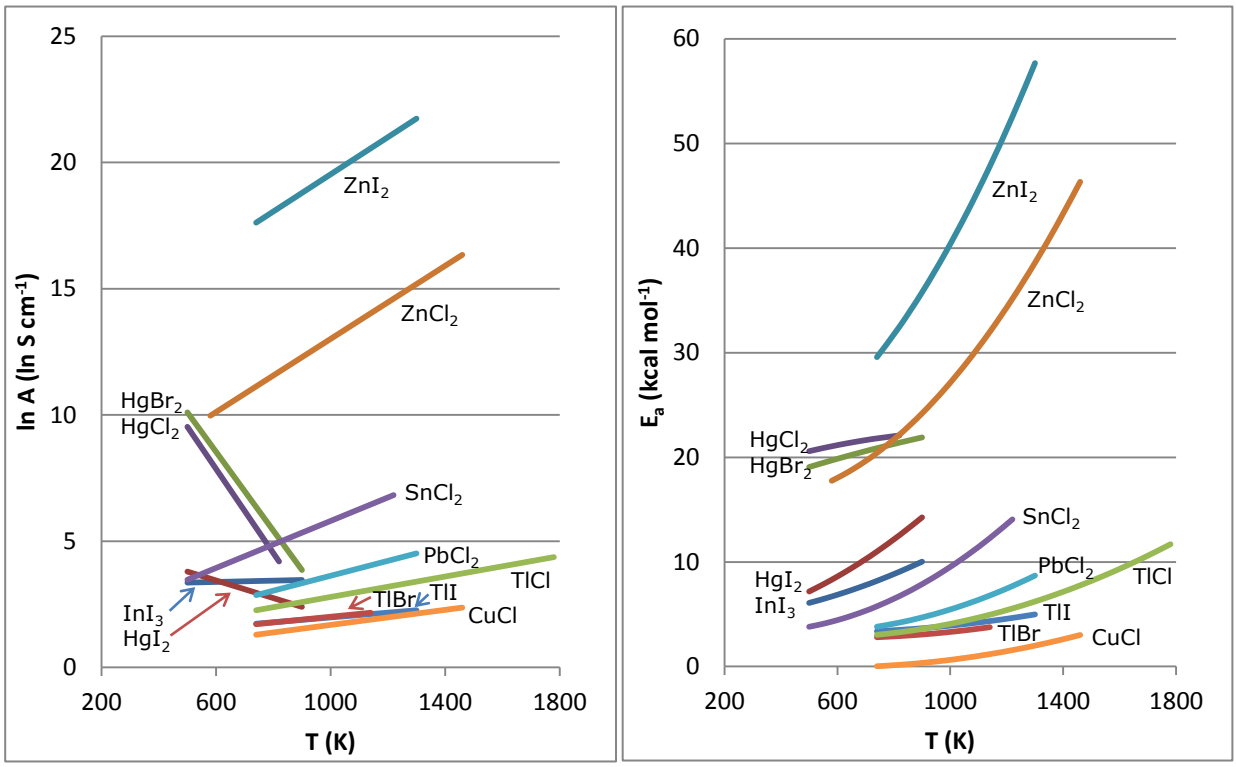

Figure 5. Results for Arrhenius parameters ln A (left) and E_a (right) for the specific conductivity of 12 molten halides, from fitting to known experimental data according to the recipe give in the text.

TABLE II. Molten salt parameters and coefficients for specific conductivity, from fitting to experimental data in Figures 3 and 4.[a]

Salt	σ_{max}	a	b	c	d0	d1	e0	e1	e2
InI_3	0.1201	0.003163	3.061	2120	3.2	0.0003	4.2	0.0003	0.0000068
HgI_2	0.03545	0.009188	4.603	1716	5.5	-0.0035	3.4	0.0019	0.0000113
$HgBr_2$	0.000406	0.014280	12.49	7222	17.9	-0.0156	14.4	0.0108	-0.0000026
$HgCl_2$	0.0000919	0.014200	12.24	8164	17.9	-0.0167	16.2	0.0112	-0.0000049
ZnI_2	0.5864	0.007049	16.30	10050	12.2	0.0074	20.0	-0.0082	0.0000286
$ZnCl_2$	1.4617	0.003855	12.06	8852	5.8	0.0072	17.6	-0.0125	0.0000220
TlI	1.7385	0.000460	2.467	1993	1.0	0.0009	4.0	-0.0029	0.0000028
TlBr	2.237	0.000481	2.707	1882	0.9	0.0011	3.7	-0.0036	0.0000032
TlCl	2.91	0.000750	3.569	2081	0.8	0.0020	4.1	-0.0056	0.0000055
$SnCl_2$	2.81	0.001755	4.995	2234	1.1	0.0047	4.4	-0.0076	0.0000127
$PbCl_2$	3.34	0.001023	4.397	2489	0.7	0.0030	4.9	-0.0074	0.0000079
CuCl	3.938	0.000478	2.443	600.9	0.2	0.0015	1.2	-0.0045	0.0000039

[a] Units: σ (S cm^{-1}), a (K^{-1}), b dimensionless, c (K), d_0 dimensionless, d_1 (K^{-1}), ε_0 (kcal mol^{-1}), ε_1 (kcal mol^{-1} K^{-1}), ε_2 (kcal mol^{-1} K^{-2}).

Acknowledgments

The work was supported by the Natural Sciences and Engineering Research Council (Discovery Grant 238871-2012), with supercomputer funding from the Canada Foundation for Innovation (Leading Edge Fund 2009, grant 21625), and the Government of Saskatchewan Innovation and Science Fund. The Laboratory of Computational Discovery (Robert Cowles, sysadmins) is thanked for supercomputer upkeep.

References

1. L. F. Grantham and S. J. Yosim, *J. Phys. Chem.* **67**, 2506 (1963).
2. L. F. Grantham and S. J. Yosim, *J. Chem. Phys.* **45**, 1192 (1966).
3. L. F. Grantham and S. J. Yosim, *J. Phys. Chem.* **72**, 762 (1968).
4. A. J. Darnell, W. A. McCollum, and S. J. Yosim, *J. Phys. Chem.* **73**, 4116 (1969).
5. G. J. Janz and J. D. E. McIntyre, *Ann. N. Y. Acad. Sci.* **79**, 790 (1960).
6. G. Treiber and K. Tödheide, *Ber. Bunsenges. Phys. Chem.* **77**, 540 (1973).
7. A. T. Clay, C. M. Kuntz, K. E. Johnson, and A. L. L. East, *J. Chem. Phys*. **136**, 124504 (2012).
8. C. M. Kuntz and A. L. L. East, in "Molten Salts and Ionic Liquids 18," *ECS Trans.* **50**(11), 71 (2012).
9. G. Kresse and J. Hafner, *Phys. Rev. B* **47**, 558 (1993).
10. G. Kresse and J. Furthmüller, *Phys. Rev. B* **54**, 11169 (1996).
11. G. Kresse and J. Hafner, *J. Phys.: Condens. Matter* **6**, 8245 (1994).
12. G. Kresse and D. Joubert, *Phys. Rev. B* **59**, 1758 (1999).
13. S. Nosé, *J. Chem. Phys.* **81**, 511 (1984).
14. A. R. Leach, *Molecular Modelling: Principles and Applications*, 2nd ed., Pearson, Harlow, UK (2001).
15. J. P. Perdew, J. A. Chevary, S. H. Vosko, K. A. Jackson, M. R. Pedersen, D. J. Singh, and C. Fiolhais, *Phys. Rev. B* **46**, 6671 (1992).
16. S. Grimme, *J. Comp. Chem*. **27**, 1787 (2006).
17. G. J. Janz, *J. Phys. Chem. Ref. Data* **17**, Supplement No. 2 (1988).
18. W. Humphrey, A. Dalke, and K. Schulten, *J. Molec. Graphics* **14**, 33 (1996).
19. G. J. Janz and J. D. E. McIntyre, *J. Electrochem. Soc.* **109**, 842 (1962).
20. G. J. Janz and D. W. James, *J. Chem. Phys.* **38**, 905 (1962).
21. A. B. Salyulev and A. M. Potapov, *J. Chem. Eng. Data* **60**, 484 (2015).
22. P. L. Spedding, *Electrochim. Acta* **18**, 111 (1973).